

First principles prediction of the solar cell efficiency of chalcopyrite materials AgMX_2 ($\text{M}=\text{In}, \text{Al}$; $\text{X}=\text{S}, \text{Se}, \text{Te}$)

GM Dongho-Nguimdo^{a,*}, Emanuel Igumbor^a, Serges Zambou^b, Daniel P. Joubert^c

^a*School of Interdisciplinary Research and Graduate Studies, University of South Africa, Pretoria, South Africa*

^b*Tampere University, Division of Electronics and Telecommunications, Korkeakoulunkatu 3, FI-33720 Tampere, Finland*

^c*The National Institute for Theoretical Physics, School of Physics and Mandelstam Institute for Theoretical Physics, University of the Witwatersrand, Johannesburg, Wits 2050, South Africa*

Abstract

Using the Spectroscopic Limited Maximum Efficiency, and Shockley and Queisser predictor models, we compute the solar efficiency of the chalcopyrites AgMX_2 ($\text{M}=\text{In}, \text{Al}$; $\text{X}=\text{S}, \text{Se}, \text{Te}$). The results presented are based on the estimation of the electronic and optical properties obtained from first principles density functional theory as well as the many-body perturbation theory calculations. The results from this report were consistent with the experimental data. The optical bandgap was accurately estimated from the absorption spectra, obtained by solving the Bethe and Salpeter equation. Fitting the Tauc's plot on the absorption spectra, we also predicted that the materials studied have a direct allowed optical transition. The theoretical estimations of the solar cell performance showed that the efficiencies from the Shockley and Queisser model are higher than those from the spectroscopic limited maximum efficiency model. This improvement is attributed to the absorption, the recombination processes and the optical transition accounted in the calculation of the efficiency.

Keywords: Solar cell efficiency, chalcopyrites, first principles

1. Introduction

Chalcopyrite materials have recently been investigated for their potential technological applications, including the miniaturisation of electronic components and the harvesting of the solar energy [1–4]. They can be useful for application in non linear optics process including second harmonic generation [5] as well as being used as thermoelectric materials [6]. Considerable efforts have been made by researchers during the last decade to improve the performance of solar cells. In 2018, Contreras *et al.* [7] were able to achieve a 19% efficiency using a tandem of $\text{ZnO}/\text{CdS}/\text{CuInSe}_2$. Chalcopyrites are predicted to have a life-time in outer space fifty times longer than that of silicon or III-V semiconductors [8]. Furthermore, the researchers obtained a very high stability against electron and proton

irradiation in spatial applications. It is therefore important to screen other chalcopyrite materials other than the Copper-Indium-Sulphur family to ascertain the existence of high efficient solar cell materials. Nowadays, due to high improvement in code development, computational tools to perform such a study have reached the level of accuracy that allows an optimal and reliable screening. In this work, we focus on two families of chalcopyrites, namely the AgMX_2 ($\text{M}=\text{In}, \text{Al}$; $\text{X}=\text{S}, \text{Se}, \text{Te}$). The direct bandgap of the AgMX_2 could be an advantage in the solar cell manufacturing. In addition, wide Reports have shown that properties such as the structural stability, size of the and nature (whether it is direct or indirect) of the bandgap, dielectric function, energy loss and absorption coefficient of a material are the important parameters which are used to predict a given material as good solar cell absorber. Theoretical efficiency calculation is a step ahead of the first principles methods in the search for potential solar cell materials. Numerous predictor models including the Shockley

*Corresponding author

Email address: donghomoise@gmail.com (GM Dongho-Nguimdo)

and Queisser (SQ) [9], Spectroscopic Limited Maximum Efficiency (SLME) [10] and Spectroscopic limited practical efficiency (SLPE) [11] have been used to tackle this problem. In this work, we use the SQ and SLME models to show that the efficiency of the studied materials does not only depend on the bandgap, but also the physics of the absorption and the recombination processes as well as the nature of the dipole transition. The outline of this paper is as follows: in Section 2, computational details are presented, Section 3 is dedicated to the electronic and the optical properties of the materials, in Section 4 we present the result of the theoretical efficiency calculations of the materials and the work is summarized in Section 5.

2. Computational details

2.1. first principles calculations

The results of this work were performed by means of density functional theory as implemented in the Vienna *ab-initio* Simulation Package (VASP) [12]. Electron-ion interaction was mimicked by the projector-augmented wave formalism [13]. Since our main interest is not on the structural parameters, we used already optimized structural parameters from previous studies [14, 15] where the generalised gradient approximation (GGA) in the revised Perdew-Burke-Ernzerhof version for solids (PBEsol) [16] was used as exchange-correlation functional. Convergence tests showed that the Monkhorst-Pack [17] \mathbf{k} -points mesh of $7 \times 7 \times 7$ with an energy cut-off of 550 eV were sufficient for sampling the Brillouin zone. The geometric structures were relaxed until the final change in the total energy was less than 10^{-5} eV and the forces acting on the atoms were relaxed to below 0.001 eV/Å. Accurate description of the electronic properties is important for calculating the optical properties. We first used a single short GW [18] also known as G_0W_0 , where the quasi-particle energies are from one GW iteration follow by a semi self-consistent GW_0 where only the Green's function is updated. In the G_0W_0 calculations, the quasiparticles energies, $\epsilon_{n\mathbf{k}}^{QP}$, are solution of the linear equation obtained by a Taylor expansion of the self-energy, Σ , around the DFT energies and all the off-diagonal matrix elements are neglected [19]:

$$\epsilon_{n\mathbf{k}}^{QP} = \epsilon_{n\mathbf{k}} + Z_{n\mathbf{k}} [Re\Sigma_{n\mathbf{k}}(\epsilon_{n\mathbf{k}}) - V_{n\mathbf{k}}^{xc}], \quad (1)$$

where $\epsilon_{n\mathbf{k}}$, $\Sigma_{n\mathbf{k}}$, $V_{n\mathbf{k}}^{xc}$ and $Z_{n\mathbf{k}}$ are the Kohn-Sham energies, the diagonal matrix element of Σ , the exchange-correlation potential and the renormalization factor, respectively. In practice, the Kohn-Sham eigenstates and eigenenergies in the calculation of $\epsilon_{n\mathbf{k}}^{QP}$ according to Equation(1) are usually taken from either the Hartree-Fock, a GGA, the local density approximation (LDA) or an hybrid functional initial calculation. In order to increase the accuracy of our calculations, we used the hybrid functional (HSE06) exchange-correlation to obtain $\epsilon_{n\mathbf{k}}$. This method helps to capture some errors such as wrong hybridization of orbitals, localization and delocalization errors encounter in GGA and LDA. The absorption coefficient is calculated by using the many-body perturbation theory at the Bethe and Selpeter level [20, 21] built on top of the GW_0 . Hence, the two particles interaction kernel is constructed and the BSE equation is solved in the Tamn-Dancoff approximation [22]. After a set of convergence test, we set the following: the number of additional empty bands to 1008, the energy cutoff for the response function to 300 eV and the number of frequency grid points to 192 for the semi self-consistent calculations. Ten occupied and unoccupied orbitals were included in the BSE calculation in order to get accurate positions of the absorption peaks.

2.2. The SQ and the SLME models

Using the first principles calculation method, the solar cell performances were calculated through the SQ and SLME models. The efficiency η , of a solar cell is the ratio of the maximum power delivered by the cell (P_{max}) and the incident solar power striking on the cell (P_{in}): $\eta = P_{max}/P_{in}$. In the SQ model, it is assumed that each photon with energy above the bandgap of the absorber produces an electron-hole pair. Hence, the maximum output per unit area per unit time can be expressed as

$$P_{max} = E_g N_{ph} \quad (2)$$

where E_g is the bandgap of the absorber and N_{ph} is the number of incident photon per unit area per unit time with energy above E_g . At a first approximation, the N_{ph} can be calculated using the Planck equation [23]. However, for a more reliable estimation, a common standard solar spectra model used as reference to allow comparison of solar cell models and devices is the air mass 1.5 global spectrum referred to as AM1.5G spectrum [24, 25].

The AM1.5G accounts for the relative path length taken by the sun's rays through the atmosphere before reaching the ground [26, 27]. Considering that all electron are not always automatically converted into current due to the recombination process, the net current is given by [28, 29]:

$$J = J_{sc} - J' \left[e^{(qV/k_B T_c)} - 1 \right], \quad (3)$$

where k_B , T_c , V , and q are the Boltzmann constant and the temperature of cell, the current voltage delivered by the module, and the electron charge, respectively. J_{sc} is the short circuit current, and J' is the current recombination rate. Contrary to the SQ model, the SLME model accounts for the photon absorptivity $a(E)$ whereby J' is calculated by

$$J' = \beta \int_0^\infty \varepsilon(E) N_{ph}(E, T_c) dE, \quad (4)$$

where $\varepsilon(E)$ is the emittance and β is a coefficient proportional to the fraction of the radiative electron-hole recombination current. According to the ‘‘principle of detailed balance’’ [9], absorptivity and emittance are equal and defined as $a(E) = 1 - e^{2\alpha(E)L}$ where L is the thickness of the absorber and $\alpha(E)$ the absorption coefficient from first principal calculations.

3. Electronics and optical properties

Table 1: The results of the structural parameters adapted from Ref. [14, 15], comparison with experimental data is also provided.

Materials	Functional	a(Å)	c/a	$V_0(\text{\AA}^3)$	$B_0(\text{GPa})$
AgAlTe ₂	PBEsol	6.31	1.906	29.91	49.83
	Exp.	6.29	1.880	29.31	-
AgAlSe ₂	PBEsol	5.91	1.866	24.00	61.23
	Exp.	5.95	1.806	23.83	-
AgAlS ₂	PBEsol	5.66	1.822	20.69	73.78
	Exp.	5.72	1.770	20.86	-
AgInS ₂	PBEsol	5.80	1.653	23.86	62.40
	Exp.	5.81	1.929	24.17	62

We calculated the size and the nature of the bandgap using the optimized structural parameters as shown in Table 1 as well as the experimental parameters. In this report, Table 2 lists the results as obtained from our theoretical calculations, other theoretical results as well as the experimental results. The results show that the bandgaps obtained

using the PBEsol are underestimated. This corroborate the results of LDA and PBE functionals, which are known to underestimate the bandgap of materials. In contrast, the results from the modified Becke-Johnson (MBJ) which is a metaGGA functional are already in the range of the experimental results despite the relatively low computational time [30]. The hybrid functional HSE06 slightly overestimates the bandgap by an average of 4.72%. However, the single short GW results are not close to the experimental data despite using the HSE06 eigenvalues as initial input and a large number of empty bands for those calculations. For example, the G_0W_0 predicts a bandgap of 2.12 and 1.5 eV for AgAlSe₂ and AgInS₂, respectively, while their experimental values are in that order 2.55 eV and 1.86 eV. The MBJ results are much improved than those from G_0W_0 calculations. G_0W_0 has a deficiency in

Table 2: Results of bandgaps using different functionals. MBJ (modified Becke-Johnson) is a metaGGA exchange-correlation functional. Comparison with experimental data is also provided. All the materials are predicted to have a direct bandgap. b =Ref. [14] and c =Ref. [15].

Materials	G_0W_0	GW_0	Exp ^{b,c}	HSE06 ^b	MBJ ^c	PBEsol ^b
AgInS ₂	0.92	1.90	1.86	1.92	1.73	0.27
AgAlS ₂	2.67	3.21	3.13	3.34	3.15	1.83
AgAlSe ₂	2.12	2.46	2.55	2.70	2.38	1.11
AgAlTe ₂	2.08	2.22	2.27	2.34	2.14	1.03

predicting chalcopyrite bandgaps accurately. Similar discrepancies were found in Ref. [31] for the band structure and optical properties of CuGaS₂. It was attributed to the fact that an important contribution to the Cu- d orbitals at the upper most valence band leads to a strong hybridisation with the Ga- p orbitals. Furthermore, Similar results were reported by S. Botti in the case of CuInS₂ and CuInSe₂ [32] where the author obtained a bandgap of 0.28 and 0.25 eV, respectively against experimental bandgap of 1.54 eV and 1.05 eV. In this study, since the materials are from the same family of chalcopyrites, we argue that this underestimation of the bandgap by G_0W_0 probably originated from its inability to capture the p - d hybridisation. We then went a step forward by employing a semi self-consistent GW calculation (GW_0) where the screened Coulomb interaction W_0 remains at the random phase approximation (RPA) level and the Green's function updated by using the quasiparticle energy from the single shot calculation. The results

of the GW_0 are very close to the experimental results. For instance, a bandgap of 2.21 and 1.9 eV were predicted for $AgAlTe_2$ and $AgInS_2$ while their experimental values are 2.27 and 1.86 eV, respectively. It is important to point out that all calculations predict a direct bandgap for all the materials irrespective of the functional used.

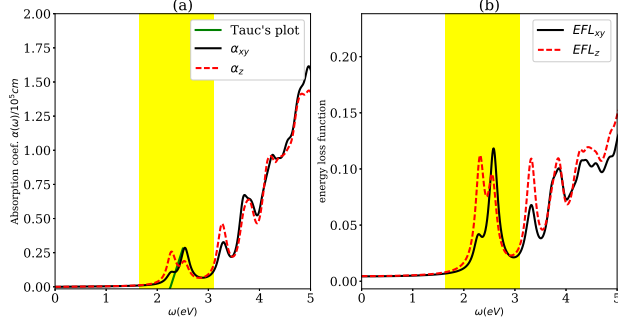


Figure 1: Plots showing (a) average absorption spectra and (b) the energy loss function of $AgAlSe_2$ material. The shaded region represents the visible range of light (1.65-3.1 eV)

Figure 1-a displays the absorption spectra $\alpha(\omega)$ and energy loss function from BSE calculations built on top of the semi self-consistent GW_0 . The shaded region indicated the visible range where photon are absorbed. Because of the anisotropy nature of the materials as depicted in Figure 2, we plotted the absorption and the energy loss function (ELF) perpendicular to xy plane and parallel to the z direction. These spectra are similar to those from chalcopyrites of $CuInS_2$ and $CuGaS_2$ from Ref. [3, 4, 33] where theoretical and experimental techniques were used. This trend is also similar for other materials in this present report. For instance, the onset of absorption in the visible range is at 2.05 and 1.92 eV along the perpendicular(\perp) and parallel(\parallel) direction, respectively. Two sharp absorption peaks appear in the visible range in each direction. The maximum occurs 2.56 and 2.28 eV for an absorption of $0.28 \times 10^5 \text{ cm}^{-1}$ and $0.25 \times 10^5 \text{ cm}^{-1}$ along the \perp and \parallel direction, respectively. The $AgInS_2$ has the highest absorption in the visible range suggesting it could make a better solar materials than the others. It is worth pointing out that for all the compounds under investigation, these peaks occur at an energy lower that the fundamental bandgap. Hence, attesting the fact that our BSE calculations were able to capture the electron-hole interaction unlike the GW and the traditional

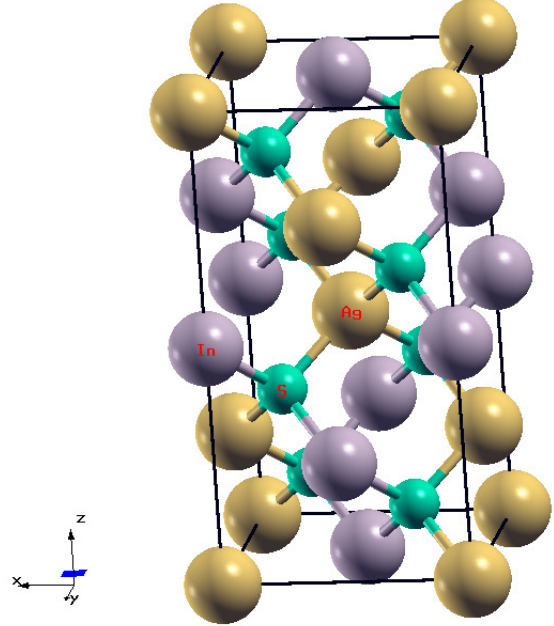


Figure 2: Illustration of the chalcopyrites structures ($a = b \approx c/2$). The xy plane is the perpendicular (\perp) while z is the parallel (\parallel) direction.

DFT functionals. We also calculated the EFL of the structures. From Figure 1-b, we can observed that the ELF has plasmon peaks at the visible range. The position of the plasmon peaks shift toward lower energy in the structure as one moves down the chalcogenide group in the periodic table.

4. Solar cell performance

In this section, we used both the SQ and SLME to estimate the solar cells efficiency of the materials. Figure 3 shows two models of the solar spectral irradiance: the blackbody model and the AM1.5G model used as solar sources. The AM1.5G spectrum is not as smooth as the blackbody prediction since it is an average distribution of the solar radiation depending on the day, the location and the path taken from the sun to the surface of the earth.

The Shockley and Queisser limit is a classic way of predicting the efficiency of the solar cells. Here, the bandgap is the main parameter used to differentiate between the materials. It can be observed from the SQ limit efficiency with the blackbody

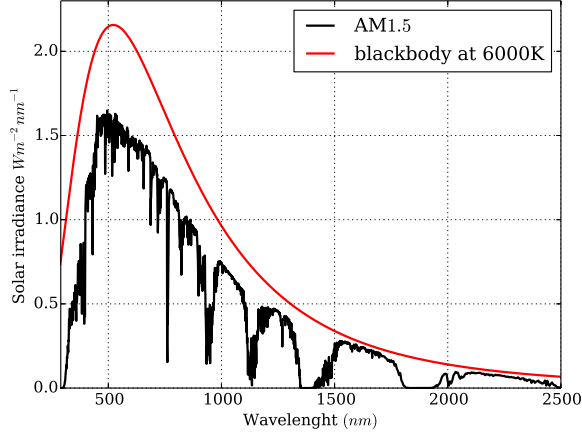


Figure 3: Blackbody and AM1.5G solar spectral intensity.

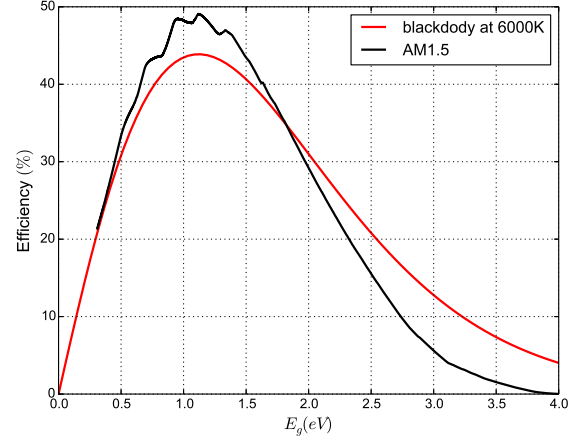


Figure 4: Comparison between the blackbody at 6000 K and the AM1.5G efficiency limit.

(BB) spectra in Figure 4 that the maximum efficiency is about 43.87% for an energy of 1.12 eV. It suggests that the best solar absorbers should be those with bandgap in that range and this may justify why the existing technologies in photovoltaic are almost all based on silicon. We also notice that the maximum efficiency from the AM1.5G spectra is at 49.08%. In addition, from 1.82 eV upwards, the number of photon absorbed by solar cell is smaller than that from the blackbody model. Table 3 shows that AgAlS₂ and AgInS₂ have respectively the least and the most efficient solar absorber materials from this study. For some materials, the difference in solar efficiency between the two solar models is important. For instance, there is a 66.6% difference between the BB and the AM1.5G solar irradiance model in the case of AgAlS₂. An

Table 3: solar efficiency(%) from SQ and SLME models using the BB and the AM1.5G spectrum

Materials	AgAlS ₂	AgAlSe ₂	AgAlTe ₂	AgInS ₂
SQ@BB	10.36	21.56	26.50	32.49
SQ@AM1.5G	3.46	16.26	23.08	31.65
SLME@AM1.5G	2.37	10.86	14.35	18.70

important factor to be considered while computing the efficiency of a solar cell absorber is the recombination process. Recombination happens when an excited electron in the conduction band loses energy and falls into the valance band which is neutralized by the hole. Numerous recombination processes have been inventoried including radiative and

non radiative recombination. Hence, all the generated electrons are not always converted into current and the fraction of exact current is given by Equations 3 and 4. In addition to the recombination processes, another factor which may influence the efficiency of a solar cell material is the specific shape of the absorption near the onset. In fact, having strong absorption and a direct bandgap is not a guarantee of a good solar cell material. Some materials with well positioned dipole forbidden direct transition lower than dipole allowed direct transitions might have a good efficiency [10]. Based on the nature of the transition, there are four possible types of optical transitions namely: the direct allowed(da), the indirect allowed, direct forbidden and indirect forbidden transitions. The relation between the absorption (α) and the incident photon can be used to determine the nature of the optical transition following the Tauc's relation [34]:

$$\alpha h\nu = \alpha_0 (h\nu - E_g^{opt})^n, \quad (5)$$

where E_g^{opt} is the optical gap and α_0 is the band tailing parameter. Depending on the value of the power factor n , the transition can be a direct allowed, an indirect allowed, a direct forbidden or an indirect forbidden for $n = 1/2, 2, 3/2$ or 3, respectively. From the Tauc's plot fitting of the absorption as illustrated in Figure 1, we found that all the materials studied have a direct allowed transition ($n = 1/2$). These findings agree with the results of Liping et al. [10] except for AgAlTe₂ where they found a direct-but-forbidden transition. The difference may probably be due to the fact that they

determined the nature of the transition from the magnitude of matrix element square. The recombination processes together with the nature of the optical transition are some of those factors that the classical SQ model does not take into consideration. Accounting for these two parameters as well as the absorptivity, the net current from Equation 3 becomes:

$$J = q \int_{E_g}^{\infty} \left[1 - e^{-2\alpha(E)L} \right] AM1.5G(E) dE - \frac{q\pi}{j_r} \left[e^{(qV/k_B T_c)} - 1 \right] \int_{E_g}^{\infty} \left[1 - e^{-2\alpha(E)L} \right] N_{ph}(E, T_c) dE, \quad (6)$$

where $j_r = e^{-\Delta/k_B T}$ defines the fraction of the radiation electron-hole recombination with $\Delta = E_g^{da} - E_g$ (da= direct allowed).

In order to get the maximum power P_{max} entering in calculation of the solar cell efficiency η , Equation 6 should be integrated numerically throughout the AM1.5G solar spectral. The maximum power is obtained at the maximum power point tracking (MPPT) of a current-voltage (J-V) characteristic for a given value of the bandgap.

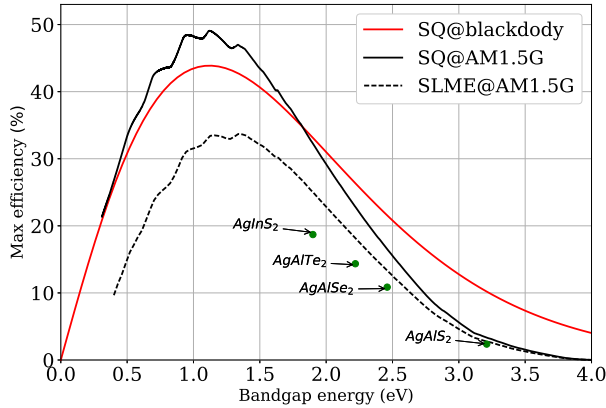


Figure 5: Efficiency vs bandgap from different models. The thickness of the thin film is set at $0.5\mu m$.

Repeating this procedure throughout the whole AM1.5G spectra leads to Figure 5 which depicts the dependence of efficiency with respect to the bandgap. The general trend is that the efficiency is lowered when accounting for the losses by recombination, the absorption spectra and the nature of the dipole transition. We obtained solar efficiencies of 2.37, 10.86, 14.35 and 18.70% for $AgAlS_2$, $AgAlSe_2$, $AgAlTe_2$ and $AgInS_2$, respectively. Recall that the absorption $\alpha(E)$ entering in the calculation of absorptivity $a(E)$ was obtained at the BSE level of the approximation while the BSE calculations were built on top of the semi self-consistent

GW approximation. There is not any previous work for the $AgAlX_2$ family, but a previous study on $AgInS_2$ predicted an efficiency about 20% [10, 28]. There is a difference of about 1% which could be attributed to different calculation methods. For instance, we used relaxed lattice parameters whereas according to Ref. [10], the experimental lattices parameters were used. It is known that the bandgap chalcopyrites strongly depends on the internal structural parameters such as the anion displacement and the tetragonal distortion. Moreover, their absorption was obtained from HSE06 calculation with a scissor operator added to improve the bandgap and the excitonic effect was not taken into consideration. Overall, the efficiency of the compounds of interest increases as the bandgap decreases for both the SQE and SLME. The low efficiency of $AgAlS_2$ relatively to others studied materials suggests that it cannot be considered for single junction solar cell absorber.

5. Conclusion

We have reported the results of the solar cell efficiency of $AgMX_2$ chalcopyrite materials based on the optical and electronics properties from first principles calculations. Since G_0W_0 underestimates the bandgaps, we circumvented this problem by performing a semi self-consistent GW calculations for all the materials in this study. These results predicted that the bandgap of $AgInS_2$, $AgAlS_2$, $AgAlSe_2$ and $AgAlTe_2$ to be 1.9, 3.21, 2.46 and 2.22 eV, respectively. In order to accurately estimate the optical absorption in the materials studied, BSE equation in the Tamn-Anaconda approximations was used. We found that all the materials have a direct allowed dipole transition by means of the Tauc's plot fitting of the absorption spectra. The classic SQ and SLME models were used for the calculation of the solar performance. We found that for a given absorber, the results of the SQ are relatively higher than those of the SLME. This is due to the fact that the SQ model only accounts for the bandgap neglecting the recombination process, the absorption as well as the optical transition. We finally predicted that the $AgInS_2$ with 24.87% and $AgAlS_2$ with 2.37% have respectively the highest and the lowest solar cell efficiency.

Acknowledgements

The Centre for High Performance Computing (CHPC), Cape Town-South Africa is Acknowledged for the computational resources. The authors are grateful to the University of South Africa for financial support.

References

- [1] B. Xu, H. Han, J. Sun, and L. Yi *Physica B: Condensed Matter*, vol. 404, no. 8, pp. 132–1331, 2009.

- [2] A. Zunger and J. Jaffe *Phys. Rev. Lett.*, vol. 51, no. 8, p. 662, 1983.
- [3] J. Koskelo, J. Hashemi, S. Huotari, and M. Hakala, "First-principles analysis of the intermediate band in $\text{CuGa}_{1-x}\text{Fe}_x\text{S}_2$," *Phys. Rev. B*, vol. 93, p. 165204, Apr 2016.
- [4] M. Alonso, K. Wakita, J. Pascual, M. Garriga, and N. Yamamoto, "Optical functions and electronic structure of CuInSe_2 , CuGaSe_2 , CuInS_2 , and CuGaS_2 ," *Physical Review B*, vol. 63, no. 7, p. 075203, 2001.
- [5] G. D. Boyd, E. Buehler, F. Storz, and J. Wernick, "Linear and nonlinear optical properties of ternary a ii b iv c 2 v chalcopyrite semiconductors," *Quantum Electronics, IEEE Journal of*, vol. 8, no. 4, pp. 419–426, 1972.
- [6] A. Yusufu, K. Kurosaki, A. Kosuga, T. Sugahara, Y. Ohishi, H. Muta, and S. Yamanaka, "Thermoelectric properties of $\text{Ag}_{1-x}\text{GaTe}_2$ with chalcopyrite structure," *Applied Physics Letters*, vol. 99, no. 6, p. 061902, 2011.
- [7] M. A. Contreras, B. Egaas, K. Ramanathan, J. Hiltner, A. Swartzlander, F. Hasoon, and R. Noufi, "Progress toward 20% efficiency in $\text{Cu}(\text{In}, \text{Ga})\text{Se}_2$ polycrystalline thin-film solar cells," *Progress in Photovoltaics: Research and applications*, vol. 7, no. 4, pp. 311–316, 1999.
- [8] K. P. O'Donnell, *Semiconductor spectroscopy and devices*, Accessed May 2014. <http://ssd.phys.strath.ac.uk/index.php/>.
- [9] W. Shockley and H. J. Queisser, "Detailed balance limit of efficiency of p-n junction solar cells," *Journal of applied physics*, vol. 32, no. 3, pp. 510–519, 1961.
- [10] L. Yu and A. Zunger, "Identification of potential photovoltaic absorbers based on first-principles spectroscopic screening of materials," *Physical review letters*, vol. 108, no. 6, p. 068701, 2012.
- [11] J. Qian, Y. Liu, J. Song, L. Liu, B. Xu, G. Chen, and W. Tian, "Spectroscopic limited practical efficiency (SLPE) model for organometal halide perovskites solar cells evaluation," *Organic Electronics*, vol. 59, pp. 389–398, 2018.
- [12] G. Kresse and J. Furthmüller, "Software VASP," *Phys. Rev. B*, vol. 54, no. 11, p. 169, 1996.
- [13] G. Kresse and D. Joubert, "From ultrasoft pseudopotentials to the projector augmented-wave method," *Phys. Rev. B*, vol. 59, no. 3, p. 1758, 1999.
- [14] G. M. Dongho Nguimdo and D. P. Joubert, "A density functional (PBE,PBEsol,HSE06) study of the structural, electronic and optical properties of the ternary compounds AgAlX_2 ($X = \text{S}, \text{Se}, \text{Te}$)," *Eur.Phys. J. B*, vol. 88, no. 5, 2015.
- [15] G. M. Dongho Nguimdo, G. S. Manyali, A. Mahmud, and D. P. Joubert, "Structural stability and electronic properties of AgInS_2 under pressure," *Eur. Phys. J. B*, vol. 89, no. 4, pp. 1–9, 2016.
- [16] J. P. Perdew, A. Ruzsinszky, G. I. Csonka, O. A. Vydrov, G. E. Scuseria, L. A. Constantin, X. Zhou, and K. Burke *Phys. Rev. Lett.*, vol. 100, p. 136406, 2008.
- [17] H. J. Monkhorst and J. D. Pack, "Special points for brillouin-zone integrations," *Phys. Rev. B*, vol. 13, no. 12, p. 5188, 1976.
- [18] M. Shishkin and G. Kresse *Phys. Rev. B*, vol. 75, no. 23, p. 235102, 2007.
- [19] M. S. Hybertsen and S. G. Louie, "Electron correlation in semiconductors and insulators: Band gaps and quasiparticle energies," *Phys. Rev. B*, vol. 34, pp. 5390–5413, Oct 1986.
- [20] E. Salpeter and H. A. Bethe, "A relativistic equation for bound-state problems," *Phys. Rev.*, vol. 84, no. 6, p. 1232, 1951.
- [21] M. M. Broido and J. G. Taylor, "Bethe-salpeter equation," *Journal of Mathematical Physics*, vol. 10, no. 1, pp. 184–209, 1969.
- [22] M. Abdulsalam and D. Joubert, "Structural, electronic and optical properties of TcX_2 ($X = \text{S}, \text{Se}, \text{Te}$) from first principles calculations," *Computational Materials Science*, vol. 115, pp. 177–183, 2016.
- [23] A. Belghachi, "Theoretical calculation of the efficiency limit for solar cells," 2015.
- [24] K. Emery and D. Myers, "Reference solar spectral irradiance: air mass 1.5," *Center, RERD, Ed*, 2009.
- [25] Y. Jestin, "Photovoltaic solar energy," in *Comprehensive renewable energy* (A. Sayigh, ed.), ch. 1, Elsevier Science & Technology, 2012.
- [26] R. Hulstrom, R. Bird, and C. Riordan, "Spectral solar irradiance data sets for selected terrestrial conditions," *Solar Cells*, vol. 15, no. 4, pp. 365–391, 1985.
- [27] P. Altermatt, "Altermatt's lectures on photovoltaics. from [<https://www.pvlighthouse.com.au/resources>] access on [13-01-2016]," 2016.
- [28] M. Bercx, N. Sarmadian, R. Saniz, B. Partoens, and D. Lamoen, "First-principles analysis of the spectroscopic limited maximum efficiency of photovoltaic absorber layers for CuAu -like chalcogenides and silicon," *Physical Chemistry Chemical Physics*, vol. 18, no. 30, pp. 20542–20549, 2016.
- [29] Dongho-Nguimdo, *Computational study of chalcogenide based solar energy materials*. PhD thesis, 2016.
- [30] F. Tran and P. Blaha *Phys. Rev. Lett.*, vol. 102, no. 22, p. 226401, 2009.
- [31] I. Aguilera, J. Vidal, P. Wahnón, L. Reining, and S. Botti *Phys. Rev. B*, vol. 84, p. 085145, 2011.
- [32] S. Botti, "Lecture notes on electronic excitations in thin-film solar cells from restricted self-consistent GW," CEA, Orme des Merisiers September 9, 2010.
- [33] A. Soni, V. Gupta, C. Arora, A. Dashora, and B. Ahuja, "Electronic structure and optical properties of CuGaS_2 and CuInS_2 solar cell materials," *Solar Energy*, vol. 84, no. 8, pp. 1481–1489, 2010.
- [34] A. Hassanien and A. A. Akl, "Effect of se addition on optical and electrical properties of chalcogenide CdSSe thinfilms," *Superlattices and Microstructures*, vol. 89, pp. 153–169, 2016.